Density Functional Studies of Actinyl Aquo Complexes Studied Using Small-Core Effective Core Potentials and a Scalar Four-Component Relativistic Method

Grigory A. Shamov and Georg Schreckenbach*

Department of Chemistry, University of Manitoba, Winnipeg, Manitoba, Canada, R3T 2N2

Received: June 28, 2005; In Final Form: October 13, 2005

The title compounds, $[AnO_2(H_2O)_5]^{n+}$, $n = 1$ or 2 and An = U, Np, and Pu, are studied using relativistic density functional theory (DFT). Three rather different relativistic methods are used, small-core effective core potentials (SC-ECP), a scalar four-component all-electron relativistic method, and the zeroeth-order regular approximation. The methods provide similar results for a variety of properties, giving confidence in their accuracy. Spin-orbit and multiplet corrections to the An^{VI}/An^{V} reduction potential are added in an approximate fashion but are found to be essential. Bulk solvation effects are modeled with continuum solvation models (CPCM, COSMO). These models are tested by comparing explicit (cluster), continuum, and mixed cluster/continuum solvation models as applied to various properties. The continuum solvation models are shown to accurately account for the effects of the solvent, provided that at least the first coordination sphere is included. Reoptimizing the structures in the presence of the bulk solvent is seen to be important for the equatorial bond lengths but less relevant for energetics. Explicit inclusion of waters in the second coordination sphere has a modest influence on the energetics. For the first time, free energies of solvation are calculated for all six $[AnO_2(H_2O)_5]^{n+}$ species. The calculated numbers are within the experimental error margins, and the experimental trend is reproduced correctly. By comparison of different relativistic methods, it is shown that an accurate relativistic description leads to marked improvements over the older large-core ECP (LC-ECP) method for bond lengths, vibrational frequencies, and, in particular, the An^{VI}/An^{V} reduction potential. Two approximate DFT methods are compared, B3LYP, a hybrid DFT method, and PBE, a generalized gradient approximation. Either method yields An^{VI}/An^{V} reduction potentials of comparable quality. Overall, the experimental reduction potentials are accurately reproduced by the calculations.

Introduction

The chemistry of the early actinide elements is related to one of the most pressing environmental challenges of our time, the radioactive waste and contamination that have resulted from decades of atomic weapons production and nuclear power generation.

Environmental actinide chemistry will almost always involve the aqueous phase, and the aquo complexes of the actinides can be considered as the prototypical environmental species. Consequently, they have attracted quite a bit of attention, both, on the experimental[1−18] and theoretical[9,11,17,19−34] sides.

In the higher oxidation state of the actinide element (An^{V}, An^{VI}), the stable actinyl unit AnO_2^{n+}, $n = 1$ or 2 and An = U, Np, and Pu, is most often formed. Various ligands can coordinate to the equatorial plane of the molecule. In this article, we will investigate the pentaaquo complexes of uranyl, neptunyl, and plutonyl, $[AnO_2(H_2O)_5]^{n+}$.

Previously,[20] we have investigated these same species using relativistic density functional theory (DFT). DFT[35] is the method of choice for a large fraction of theoretical actinide molecular science because it accounts for the all-important electron correlation in an efficient manner.[36] In that earlier study,[20] we were successful in predicting properties such as the equatorial coordination number or the vibrational frequencies. On the other hand, we have also studied the reduction potential from the An^{VI} to the An^{V} species.[20] Upon including *all of* (scalar) relativity, correlation, bulk solvation, spin−orbit, and multiplet effects, we were able to predict the relative reduction potential correctly (i.e., Np > Pu > U). However, our absolute calculated values were uniformly too high by some 2−3 eV as compared to experiment. At the time, we were unable to draw a firm conclusion regarding the reason for this discrepancy since a number of approximations could have been responsible.

Indeed, at least four different levels of approximation are required in applying quantum chemistry to molecules of the actinides, viz., (i) an approximate relativistic method, (ii) approximations for the treatment of the electron−electron correlation (which, in the case of DFT, amounts to the choice of an approximate XC functional), (iii) solvent models for the bulk solvent environment beyond the first coordination sphere, and (iv) for large ligands that might not be amenable to computational studies, the choice of truncated model systems. Here, we have used the actinyl water complexes to test the first three approximations. We have calculated a number of molecular properties and compared them to experiment where possible, thus evaluating the different levels of approximation. In particular, we have studied bond lengths, vibrational frequencies, coordination numbers, free energies of solvation, and An^{VI}/An^{V} reduction potentials.

Regarding the relativistic approximation, we used standard "large-core" effective core potentials[37] (LC-ECPs) on the actinide element as the relativistic approximation in our earlier study.[20] These ECPs treat 78 electrons as core, and the remaining

* To whom correspondence should be addressed. E-mail: schrecke@cc.umanitoba.ca.

10.1021/jp053522f CCC: $30.25
Published on Web 11/12/2005

14 (uranium), 15 (neptunium), or 16 (plutonium) electrons as valence. More recently though, evidence has been mounting in the literature that "small-core" ECPs[38] (SC-ECP, treating only 60 electrons as core), although computationally more demanding due to the larger number of valence electrons, have a tremendous effect on the calculated properties of actinide molecules. Thus, SC-ECP calculations give much closer agreement with experiment for a number of molecular properties, including geometries,[39,40] vibrational frequencies,[39,40] or ligand NMR chemical shifts.[41−43] Most recently, Batista et al.[44] have shown that the use of SC-ECPs, along with the B3LYP exchange-correlation (XC) functional,[45−47] gives excellent results for the first bond dissociation energy of UF_6. The LC-ECP−B3LYP energy is much further off as compared to experiment. Batista et al.[44] have also discussed possible reasons for the strong influence of the—seemingly core-type—orbitals that are neglected in the LC-ECP approach but included in the valence space of the SC-ECP approach.

As was shown in our earlier paper,[20] solvation effects play an important role in the An^{VI}/An^{V} reduction potentials of actinyl aquo complexes. Thus, the accuracy of the solvation models employed should be tested.

The most commonly used models for the description of solvation effects are cluster models (where solvent molecules are treated explicitly) and continuum models. The solvation of actinyl complexes has been studied in several articles.

Moskaleva et al.[33] calculated hydration energies of uranyl and protonated uranyl dications using generalized gradient approximation (GGA) density functionals and several solvation methods. They showed that the first coordination sphere of uranyl has to be included in continuum model calculations it order to obtain reliable hydration energies.

Marsden et al.[32] modeled small uranyl cation−water clusters using up to five water molecules at the MP2 level and up to eight molecules forming the first and second coordination sphere of the uranyl aquo complex with a model potential derived from ab initio results. They conducted global minimum optimization for the latter case. Interestingly, water molecules in the second coordination sphere preferred coordination to equatorial waters of the first coordination sphere over coordination to uranyl oxygens.

Infante and Visscher[48] investigated water clusters surrounding the $[UO_2F_4]^{2-}$ and $[UO_2F_4(H_2O)]^{2-}$ complexes. They used a combined quantum-mechanics/molecular mechanics (QM/MM) approach based on GGA-DFT calculations. Up to 72 water molecules were included in the outer coordination spheres of the complexes, although no global minimum search has been done. The best results were obtained when 11 of the second coordination sphere water molecules were included in the QM region. The authors reported significant charge transfer from the complexes to the second coordination sphere waters. This charge transfer favors heptacoordination for uranium over hexacoordination.[48]

In summary, it seems that the effects of the bulk solvent can be adequately grasped with continuum models, as long as the first coordination sphere of the actinyl cation is provided explicitly. On the other hand, charge transfer and polarization effects were shown to be of importance. They can be described with cluster solvation models, by explicit inclusion of the second coordination sphere. Thus, we are going to test continuum, cluster, and mixed cluster-in-continuum solvation models for the actinyl aquo complexes.

This paper is organized as follows. The next section provides details of the computational methods. A section dedicated to the presentation and discussion of the results follows this. We begin this section with a discussion of structures and frequencies. Next, we compare implicit and explicit solvation and discuss free energies of solvation—a more stringent test of the solvation model. Finally, we discuss the An^{Vi}/An^{V} reduction potential that is the least straightforward of all the properties discussed here. The final section of the paper provides a summary and conclusions.

Computational Methods

Calculations were performed using three different programs, Gaussian03[49] (G03), the Amsterdam Density Functional code[50−52] (ADF), and Priroda.[53−55] All calculations were done with DFT in the form of either the well-established hybrid B3LYP[45−47] or the pure GGA PBE[56] XC functionals. The PBE functional was chosen because it is known[35] to be one of the most accurate GGA functionals available. Harmonic vibrational frequencies were used to verify the nature of the stationary point when performing gas-phase geometry optimizations. They were also used for the thermochemistry. The actinyl water complexes we study in the present work have many low-lying frequencies. In the harmonical approximation, this might be a source of some error in the calculation of the entropies and free energies. However, estimation of the anharmonic effects is computationally very demanding, and therefore left beyond the scope of our paper. There is evidence,[57] however, that anharmonic corrections to the zero-point energies contributions to the binding energy of water clusters are rather small. Thus, neglecting them—as we did for our explicit solvation calculations (see below)]—would not lead to significant errors.

In Gaussian, relativistic effects were included by replacing the core of the actinide element with a SC-ECP according to Küchle et al.[38] We are thus treating 60 electrons as core and the remainder as part of the variational valence space. Following earlier studies,[58] we used the actinide basis sets that have been published for the SC-ECP[38] but completely uncontracted and with the most diffuse s, p, d, and f functions removed. The 6-31g(d) all-electron basis sets were used for ligand atoms. For all the G03 calculations, "ultrafine" integration grids and tight SCF convergence criteria were used.

Priroda applies a scalar four-component relativistic method where all spin−orbit terms are separated from scalar terms[59] and are neglected.[53−55] Unless noted otherwise, we use all-electron Gaussian basis sets of double-ζ-plus-polarization (DZP) quality for the large component, and the corresponding kinetically balanced basis sets for the small component. The explicit solvation calculations for the uranium complexes have been performed with a triple-ζ-plus-polarization (TZP) basis set for the large component (accompanied again by the corresponding kinetically balanced basis sets for the small component) in order to achieve a better description of weak intermolecular interactions and reduce basis-set superposition effects. Since TZP-quality basis sets are not yet available for either Np or Pu, we have mostly used DZP basis sets, to have a consistent method for all three elements. It should be noted that both DZP and TZP yield almost similar results for selected uranium complexes.

The performance of Priroda as applied to the simulation of actinide molecules has not been evaluated in the literature in any detail. Hence, we have performed various test calculations on small molecules such as, for instance, UO_2^{2+}, UO_2F_2, UOF_4, or UF_6. In all cases, we found Priroda to be entirely reliable in that it gives essentially the same results as other codes (and thus other relativistic methods), provided the same XC functional

TABLE 1: Calculated (Gaussian SC-ECP-B3LYP and LC-ECP-B3LYP;[a] Priroda DZP Four-Component Scalar Relativistic PBE) and Experimental[b] Bond Lengths and Actinyl Frequencies of $[AnO_2(H_2O)_5]^{n+}$ Species, An = U, Np, Pu; n = 1, 2 (Bond lengths in Å, Frequencies in cm^{-1})

	$[UO_2(H_2O)_5]^{2+}$				$[NpO_2(H_2O)_5]^{2+}$				$[PuO_2(H_2O)_5]^{2+}$			
	calculated				calculated				calculated			
	SC-ECP	LC-ECP[a]	Priroda	exp[b]	SC-ECP	LC-ECP[a]	Priroda	exp[b]	SC-ECP	LC-ECP[a]	Priroda	exp[b]
R(An═O)	1.751	1.756	1.776	1.76; 1.78	1.730	1.752	1.758	1.75	1.720	1.742	1.749	1.74
R(An—O_{eq})[c]	2.486	2.516	2.472	2.41	2.470	2.50	2.457	2.42	2.466	2.485	2.453	2.41
ν_{symm}	940	908	884	870; 869	943	854	880	854; 863	912	805	855	833; 835
ν_{asym}	1032	1001	971	965; 962	1046	983	977	969	1035	951	970	
	$[UO_2(H_2O)_5]^{1+}$				$[NpO_2(H_2O)_5]^{1+}$				$[PuO_2(H_2O)_5]^{1+}$			
	calculated				calculated				calculated			
	SC-ECP	LC-ECP[a]	Priroda	exp[b]	SC-ECP	LC-ECP[a]	Priroda	exp[b]	SC-ECP	LC-ECP[a]	Priroda	exp[b]
R(An═O)	1.806	1.810	1.824		1.791	1.81	1.807; 1.810	1.83	1.776	1.808	1.796; 1.797	1.81
R(An—O_{eq})[c]	2.585	2.616	2.568		2.588	2.61	2.567	2.50; 2.52	2.577	2.61	2.567	2.47
ν_{symm}	849	840	817		842	794	809	767	824	718	798	748
ν_{asym}	913	909	875		922	904	884	824	915	871	883	

[a] Hay et al., ref 20. [b] Experimental data[1−3,6,9] cited from Hay et al.[20] [c] Average.

was used.[60,61] We intend to publish a critical evaluation of different methods as applied to actinide molecules in a separate paper.[60]

It should be noted that Priroda makes judicious use of various methods for accelerating the DFT calculations, both for SCF and geometry convergence. It is therefore a very efficient code, despite employing an all-electron four-component relativistic method and using very tight numerical integration and SCF convergence criteria.

Currently, no continuum solvation model is available in Priroda. Solvation effects have therefore been modeled using the CPCM polarized continuum solvent model[62] as implemented in the Gaussian code, unless otherwise noted. The dielectric constant for the water solvent was taken as 78.4. We calculated single-point CPCM energies at gas-phase geometries. Specifically, we used the G03-B3LYP-optimized geometries for the B3LYP-CPCM results and Priroda-PBE-optimized geometries for the G03-PBE-CPCM results. This latter procedure was chosen because of the difficulties and computational cost of achieving full geometry convergence within G03. It is fully justified because of the similarities between the PBE structures optimized with Priroda and G03.

We have tested the validity of our procedure by reoptimizing two uranyl complexes, $[UO_2(H_2O)_5]^{2+}$ and $[UO_2(H_2O)_5]^{+}$, with Gaussian03 and PBE, starting from the respective Priroda structure, and then calculating single-point energies in water solution using CPCM. This led to changes in the electronic energy in the gas phase ΔE and free energy in solution ΔG, respectively, of −0.58 kcal/mol (U^{VI}) and −0.92 kcal/mol (U^{V}) for ΔE and −1.77 kcal/mol (U^{VI}) and −0.95 kcal/mol (U^{V}) for ΔG, respectively. The respective change for the An^{VI}/An^{V} redox half reaction in solution amounts to 0.82 kcal/mol, which is much smaller than various other error sources, thus validating our approach.

Finally, some calculations were performed also with the scalar relativistic zeroeth order regular approximation (ZORA) method[63−66] as implemented in the ADF.[50−52] This was done to further estimate solvent effects. We chose an additional code for this task (i.e., ADF) because, on one hand, the COSMO solvation model[67,68] available in ADF allowed for geometry optimizations in the presence of the bulk solvent, whereas CPCM optimizations in G03 consistently failed to converge due to numerical noise or some other computational instabilities. On the other hand, we have found ZORA to be of similar quality as the other relativistic methods employed in this study.[60,61] The ADF-ZORA calculations employed the ZORA-TZP all-electron standard basis sets of ADF, a numerical integration parameter of 5.5, and the PBE XC functional. In ADF-COSMO calculations,[68] we used the Klamt atomic radii for the oxygen and hydrogen atoms,[69] and an atomic radius of 1.70 Å for the uranium atom.

TABLE 2: Calculated PBE (Gaussian SC-ECP, ADF scalar ZORA TZP, Priroda TZP and Priroda DZP Four-Component Scalar Relativistic) Bond Lengths and Actinyl Frequencies of $[UO_2(H_2O)_5]^{n+}$ Species; n = 1, 2 (Bond Lengths in Å, Frequencies in cm^{-1})

	SC-ECP	ADF ZORA	Priroda-TZP	Priroda-DZP
		$[UO_2(H_2O)_5]^{2+}$		
R(U═O)	1.771	1.776	1.778	1.776
R(U—O_{eq})[a]	2.467	2.486	2.482	2.472
ν_{symm}	887	884	897	884
ν_{asym}	981	975	991	971
		$[UO_2(H_2O)_5]^{1+}$		
R(U═O)	1.817	1.825	1.826	1.824
R(U—O_{eq})[a]	2.574	2.599	2.586	2.568
ν_{symm}	819	810	823	817
ν_{asym}	885	870	883	875

[a] Average.

The same test cases as for Gaussian03 above, the $[UO_2(H_2O)_5]^{2+}$ and $[UO_2(H_2O)_5]^{+}$ aquo complexes, were used for comparing the energy differences between ADF and Priroda optimized structures. In this case, we find differences of −0.08 kcal/mol (U^{VI}) and +0.91 kcal/mol (U^{V}) for the gas-phase energy ΔE and −1.07 kcal/mol (U^{VI}) and −0.86 kcal/mol (U^{V}) for ΔG in solvation, correspondingly. The differences are again very small. The effects of solution on the geometries and energies will be discussed further below.

In all continuum solvation calculations, vibrational contributions to the Gibbs free energy were taken from gas-phase harmonic frequency calculations on the corresponding gas-phase-optimized geometries. Moreover, for PBE calculations, values obtained with the Priroda program were used throughout since we did not recalculate frequencies for all the molecules with G03 or ADF due to the computational cost. Some examples (uranyl frequencies) given by PBE with these three different codes are provided in the Table 2.

Earlier, it was pointed out[70] that, for calculations of the thermodynamics of water molecules in water solution, the standard state might have to be modified to take into account

the reduction of its translation entropy. This can be done[70] by setting the water pressure to 1354 atm (value derived from the liquid water density of 997.02 kg/m^3) instead of 1. At 298 K, this would contribute −4.3 kcal/mol in Gibbs free energy of any reaction involving water, per single water on the left side of its equation.

All calculations have been performed using the scalar relativistic approximation, i.e., neglecting spin−orbit effects. For structures and frequencies, this is generally believed to be a valid approach.[60,61,71,72] However, neglecting spin−orbit effects is clearly insufficient in determining energetics for reactions where the formal oxidation state of the heavy metal is not constant as is the case for the reduction potentials. Moreover, while DFT is, in principle, an exact theory, approximate XC functionals currently in use do not account for multiplet effects that become relevant for f^n systems with $n > 1$. We include both effects in an ad hoc fashion using the same approach as in our previous paper[20] where corrections had been determined for PuO_2^{q+} species, $q = 1, 2, 3$ using spin−orbit configuration interaction, SO-CI. These corrections were then transferred directly to the different AnO_2^{n+}−water complexes. (This approach amounts to assuming a weak ligand field for the aquo complexes *and* transferability of the results from Hartree−Fock-based SO-CI to DFT.) The accuracy of this approach and the nontrivial problem of "double-counting" correlation effects has been discussed in our previous paper[20] where we have also compared the SO-CI results to other calculations. As the results below illustrate, it appears to be not a serious problem—although, of course, the ad hoc approach taken here is somewhat unsatisfactory from a purely theoretical point of view.

Results and Discussion

Geometries and Vibrational Frequencies. Calculated (gas-phase) geometries and actinyl frequencies of the actinyl penta-aquo complexes are compiled in Table 1 where they are also compared to the available experimental data[1−6,8,9,20] as well as to our earlier results that were obtained with the LC-ECP method.[20] As in that study, the penta-aquo complexes show geometries that are slightly distorted from C_5 symmetry, with one of the water molecules bending out of the equatorial plane. As an example, Figure 1 shows the optimized structure of $[UO_2(H_2O)_5]^{2+}$.

The axial (actinyl) bond lengths are shorter with the SC-ECP-B3LYP method than predicted by the older LC-ECP-B3LYP calculations (by up to 0.03 Å), leading to an overbinding, i.e., bond lengths that are too short. This is in contrast to earlier studies where SC-ECP calculations led to improved bond lengths (and consequently frequencies) for AnF_6 species and UF_6 derivatives.[39,40,42,44] The SC-ECP-B3LYP equatorial bond lengths, on the other hand, are closer to experiment than the older LC-ECP-B3LYP values that were overestimated by about 0.1 Å in each case.

In addition to the hybrid DFT calculations (B3LYP), we have also optimized the structures with the GGA functional PBE. In Table 1, we show results of PBE optimizations that are based on the scalar-relativistic four-component approach as implemented in Priroda.

As noted in the previous section, reoptimizing the uranyl(V) and (VI) penta-aquo complexes with either the G03-based SC-ECP-PBE or the ADF-ZORA-PBE approaches did not lead to any marked differences in energetics. Table 2 contains the corresponding gas-phase-optimized geometries and uranyl vibrational frequencies for these complexes obtained by the different PBE methods employed in this study: Gaussian03's SC-ECP, scalar ZORA (ADF), and both DZP and TZP bases with the Priroda code. Differences in uranyl frequencies never exceed 15 cm^{-1}. The methods with smaller ligand basis sets, SC-ECP and Priroda-DZP, tend to give slightly shorter U−O bond lengths than those with triple-ζ quality ligand basis sets (ADF-ZORA and Priroda-TZP). Nonetheless, the uranium-to-actinyl-oxygen distances as well as the average equatorial distances given by these methods are very close.

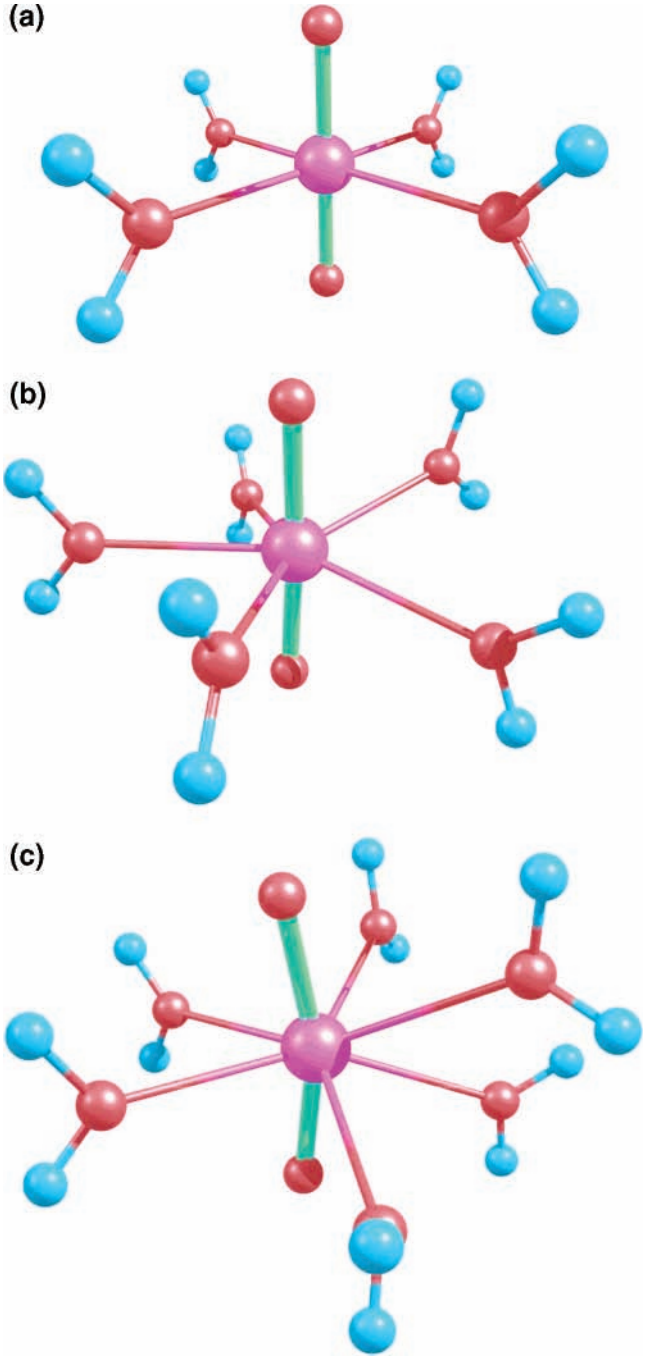

Figure 1. Optimized structures (Priroda-TZP, PBE) of (a) $[UO_2(H_2O)_4]^{2+}$, (b) $[UO_2(H_2O)_5]^{2+}$, and (c) $[UO_2(H_2O)_6]^{2+}$.

For that reason, costly reoptimizations of the Priroda PBE geometries with Gaussian or ADF have not been pursued any further in this work.

PBE-optimized structures show better agreement with experiment than SC-ECP-B3LYP-optimized structures for both the axial (actinyl) and equatorial bond lengths (Table 1). The former are elongated by about 0.03 Å (An^{VI}) and 0.02 Å (An^{V}),

TABLE 3: Calculated Geometries, Vibrational Frequencies, and Bond Orders of the Bare Actinyl Species AnO_2^{n+}

	G03 SC-ECP B3LYP			
	bond length (Å)	symmetric stretching frequency (cm^{-1})	asymmetric stretching frequency (cm^{-1})	
UO_2^{2+}	1.702	1037	1137	
UO_2^{1+}	1.746	953	1025	
NpO_2^{2+}	1.685	1031	1141	
NpO_2^{1+}	1.725	956	1039	
PuO_2^{2+}	1.683	980	1115	
PuO_2^{1+}	1.721	924	1024	
	Priroda DZP four-component scalar PBE			
	bond length (Å)	symmetric stretching frequency (cm^{-1})	asymmetric stretching frequency (cm^{-1})	An═O bond order
UO_2^{2+}	1.724	965	1060	2.53
UO_2^{1+}	1.777	896	969	2.47
NpO_2^{2+}	1.723	934	1044	2.49
NpO_2^{1+}	1.757	883	973	2.46
PuO_2^{2+}	1.713	901	1030	2.45
PuO_2^{1+}	1.743	(convergence failure)		

respectively, thus correcting the apparent overbinding of the B3LYP method. Equatorial bond lengths are, on the other hand, 0.01−0.02 Å shorter with PBE than with the SC-ECP-B3LYP method, and thus closer to experiment— although they are still longer than the available experimental values.

Calculated vibrational frequencies along the actinyl axis follow the same trend as the respective bond lengths: The new SC-ECP-B3LYP calculations show overbinding, and consequently the agreement with the available experimental data has deteriorated as compared to the older LC-ECP-B3LYP results. The PBE frequencies, on the other hand, are comparable in quality to the older LC-ECP-B3LYP values, Table 1. One should keep in mind that most of the experimental frequency data is relatively old and as such associated with a comparatively large error margin.

In going from left to right along the actinide series (i.e., from U to Np to Pu), the actinide contraction is clearly evident from the data. As has been noted earlier,[20] the actinyl bond becomes both shorter and weaker along the series, due to the decreasing size of the f orbitals and thus decreasing covalent character of the bonds.

As a minor point, we need to mention one problem with some of the Pu^{VI} calculations. For f^n species ($n \geq 1$), one would expect the n f electrons to singly occupy molecular orbitals that are essentially nonbonding f orbitals on the metal. Without considering spin−orbit, one would further expect these singly occupied molecular orbitals (SOMO) that correspond to the unpaired electrons to be the highest-occupied molecular orbitals. Careful inspection of the results show that this is, indeed, the case for all calculations except $[Pu(H_2O)_5]^{2+}$ if calculated with the SC-ECP−B3LYP approach. For this one data point only, we obtain a highly spin-polarized UHF configuration—i.e., certain occupied ligand orbitals (essentially oxygen lone pairs on the water ligands) have a higher energy than the two metal-based SOMOs. This will have *some* effect on the calculated energetics of the system. However, the effect is expected to be modest, given that the correct MO occupations are preserved— even if their ordering is slightly wrong. Interestingly, calculating the same system with the PBE approach (SC-ECP or scalar four-component) yields the correct result (that is also in line with all the other complexes) in that the two f-based SOMOs have the highest energy among occupied orbitals.

The structures and frequencies of the bare actinyl species AnO_2^{n+} (that enter the left-hand side of eq 4, see below) are summarized in Table 3 where we have also included the theoretical bond order as calculated with the Priroda code. The calculated bond lengths show again the actinide contraction in going from U to Pu, whereas frequencies and bond orders demonstrate again the trend of decreasing bond strengths along the series. Nonetheless, all six species show appreciable triple bond character for the actinyl bond. Bare actinyl species have been studied extensively by various theoretical methods (e.g., refs 19, 20, 28, 39, and 73−79). However, a detailed discussion of bare actinyls is beyond the scope of the current paper.

Equatorial Coordination Number of Uranyl(VI). It is well established, based on extended X-ray absorption fine structure, NMR, and by analogy with X-ray studies on uranyl-containing crystals, that the dominating form of the uranyl(VI) complexes in water is the pentaaquo complex.[5−9] To have the five water molecules in the first coordination shell of uranyl(VI), the free energy of the reaction 1 should be negative and the one of reaction 2 positive

$$[UO_2(H_2O)_4]^{2+} + H_2O \rightarrow [UO_2(H_2O)_5]^{2+} \quad (1)$$

$$[UO_2(H_2O)_5]^{2+} + H_2O \rightarrow [UO_2(H_2O)_6]^{2+} \quad (2)$$

Results of some previous calculations[20,25] are summarized in Table 4.

As mentioned in the Introduction, we were able to predict the correct equatorial coordination number for the U^{VI} complex using the older LC-ECP-B3LYP approach and the BSJ[80] continuum solvation model.[20] The latter was proven to be of critical importance, because gas-phase LC-ECP-B3LYP calculations predicted a negative free energy of reaction 2. However, a uranyl complex with five waters in the first and the sixth water in the second coordination sphere of the metal was found to have a lower energy than the hexa-aquo complex.[20]

Tsushima et al.[25] came to the same conclusion using the same LC-ECPs combined with the B3LYP functional and the PCM[81] continuum solvation model. While optimizations were performed with the same 6-31g* basis for the ligand atoms, they calculated energies using bigger polarized sets such as 6-311++g**. They used a supermolecule approach, comparing energies of the complexes $[UO_2(H_2O)_4](H_2O)^{2+}$ vs $[UO_2(H_2O)_5]^{2+}$ and $[UO_2(H_2O)_5](H_2O)^{2+}$ vs $[UO_2(H_2O)_6]^{2+}$, respectively. To make the numbers comparable, we derived the energies of reactions 1 and 2 from the data provided in the article[25] (Table 4). Since there is no data for isolated tetra-aquo complex available in the article, we used the energies of $[UO_2(H2O)_4](H_2O)^{2+}$ and $[UO_2(H_2O)_5](H_2O)^{2+}$ in our estimation of the energetics of eq 1 (footnote c to Table 4). If calculated that

TABLE 4: Addition of the Fifth and Sixth Water Molecule to the $[UO_2(H_2O)_4]^{2+}$ Complex: Calculated Reaction Energies in Water Solution, kcal/mol

reaction, reference	method	ΔE_{298} gas phase	ΔG_{298} gas phase	ΔG_{298}, solvation[a]		ΔG_{298}, solvation, with S_{transl} corrections applied[a]	
1, this work	SC-ECP B3LYP	−28.5	−21.5	−11.5	(−6.8)	−15.8	(−11.1)
1, this work	Priroda-DZP PBE	−24.9	−15.8	−5.5	(−0.6)	−9.8	(−4.9)
2, this work	SC-ECP B3LYP	−18.9	−4.0	−3.9	(8.2)	−8.2	(3.9)
2, this work	Priroda-DZP PBE	−16.7	−4.7	4.2	(4.0)	−0.1	(−0.3)
1, ref 20	LC-ECP B3LYP	−28.9	−19.3	−2.3		−6.6	
2, ref 20	LC-ECP B3LYP	−22.4	−9.7	5.7		1.4	
1, ref 25	LC-ECP B3LYP[b,c]	−20.1	−9.4	1.1		−3.2	
2, ref 25	LC-ECP B3LYP[b]	3.8	10.9	26.1		21.8	

[a] Values in parentheses are with COSMO-PCM solvation; for others, see text. [b] Derived from data provided in the Table 1 in ref 25. [c] Since no data is provided for $UO_2(H_2O)_4$ in ref 25, this has been calculated for tetra- and penta-aquo complexes of uranyl containing one water molecule in the second coordination sphere.

way, the free energy of reaction 1 in solution gets positive, meaning that the preferred equatorial coordination number of uranyl(VI) is four. The standard-state correction for the translation entropy of water (see the Computational Details section) decreases the free energies of reactions 1 and 2 by −4.3 kcal/mol. In this way, Tsushima et al.[25] predict the correct five-coordination (Table 4, last column).

In summary, it seems that the results are highly sensitive to various factors: the accuracy of the gas-phase calculation, the solvation method and entropy effects. In the current study, we are using a different relativistic method (SC-ECP, ZORA, or scalar four-component all-electron Priroda vs LC-ECP) and different continuum models (COSMO and CPCM). Thus, we need to make sure that, by making these modifications, we do not lose features of the previous approach that were essentially right. First, we exploited the approach from our earlier paper,[20] treating the incoming water molecule separately in the CPCM-modeled bulk water.

The complexes $[UO_2(H_2O)_4]^{2+}$ and $[UO_2(H_2O)_6]^{2+}$ were optimized in the gas phase using both G03-SC-ECP-BLYP and Priroda-TZP-PBE. The Priroda structures are shown in Figure 1. The uranyl distances for the tetra-aquo complex are 1.746 (G03) and 1.773 Å (Priroda) correspondingly; equatorial U−O bond lengths are 2.427 and 2.421 Å. The hexa-aquo complex was found to be a minimum on the potential-energy surface by both methods. It has a distorted geometry, with the water ligands bending out of the uranyl equatorial plane (Figure 1c). Priroda-TZP-PBE predicts a fairly bent geometry of the uranyl unit in that complex, with a O═U═O angle of 163.7°; similarly, G030-SC-ECP-B3LYP gives 166.6°. The uranyl distances for the hexaaquo complex are 1.758 (G03) and 1.788 Å (Priroda); the averaged equatorial bond lengths 2.547 and 2.537 Å, correspondingly. The actinyl distances increase slightly with the increase of the equatorial coordination number of uranyl(VI) from four to five to six.

The gas-phase energies provided by SC-ECP-B3LYP for the reaction 1 are in agreement with those of our earlier LC-ECP-B3LYP calculations[20] and systematically more exoenergetic than those of Tsusima et al.[25] (Table 4). Unlike the latter, inclusion of solvation effects by means of the CPCM model leads to a favorable free energy of addition of the fifth water molecule even without applying corrections for the translational enthalpy of water in water. Scalar four-component Priroda-TZP-PBE systematically underbinds as compared to B3LYP but gives the qualitatively same result.

For the process of adding the sixth water, in reaction 2, our SC-ECP-B3LYP gives gas-phase energies that are less negative than the old LC-ECP calculations.[20] However, combined with CPCM solvation, it leads to a negative free energy for reaction 2, therefore predicting the most stable coordination number to be six. Inclusion of the translation entropy correction would make it even more exothermic (Table 4, last column). Priroda-TZP calculations yield an exoenergetic ΔG_{solv}^{298} for (2) in CPCM-modeled water. This becomes thermoneutral after the entropy correction.

In summary, both SC-ECP-B3LYP and Priroda-TZP-PBE yield larger gas-phase free energies of reaction 2 as compared to the older LC-ECP calculations;[20] however, the situation in solution becomes very different. To test the influence of the particular continuum model, we also applied the COSMO-PCM solvation model[67] (Table 4, values in parentheses). COSMO-PCM differs from CPCM only with respect to the generation of the solvent-accessible surface, by employing the original Klamt radii[67] for the atoms instead of the topological VA0 model used in CPCM.[49] The results gets changed considerably again for the SC-ECP-B3LYP method, and the preferred coordination number becomes definitely five. At the same time, no significant changes occur for the Priroda-TZP-PBE calculations.

Finally, it shall be noted that, according to the data of Tsushima et al.,[25] explicit inclusion of some of the water molecules in the second coordination sphere can change things again, favoring lover coordination numbers.

Explicit Solvation and Continuum Solvation Models. As already seen in the previous section, the actinyl aquo complexes provide an excellent testing ground not only for the approximations made to describe relativity and electron correlation (discussed elsewhere in this paper) but also for the solvent model. In other words, we want to further assess whether our protocol for estimating solvent effects is adequate. (This protocol comprises gas-phase geometry optimizations of the complexes including their first coordination sphere, followed by single-point energies including CPCM or COSMO solvation. These two continuum solvation models are equivalent and differ mainly in the atomic radii used to generate the solvent-accessible surface.) We have optimized the uranyl(VI) and (V) complexes at different levels of explicit and implicit solvation.

In Tables 5 and 6, we compare the bare uranyl species $[UO_2]^{n+}$, $n = 1, 2$, the gas-phase water complexes $[UO_2(H_2O)_5]^{n+}$ (first solvation sphere included), and the latter molecules with additional k water molecules, representing the second solvation sphere, $[UO_2(H_2O)_5]^{n+}\cdot kH_2O$ ($k = 5, 7, 10,$ or 12). The $k = 7$ and 12 geometries were obtained by performing full geometry optimizations from structures that contain one second-coordination-sphere solvent (water) molecule per axial uranyl oxygen and one ($[UO_2(H_2O)_5]^{n+}\cdot 7H_2O$) or two ($[UO_2(H_2O)_5]^{n+}\cdot 12H_2O$) solvent molecules, respectively, per first-coordination-sphere water molecule. The structures for ($[UO_2(H_2O)_5]^{n+}\cdot 5H_2O$) and ($[UO_2(H_2O)_5]^{n+}\cdot 10H_2O$) were obtained in a similar fashion but with no waters attached to the uranyl oxygens, see below.

TABLE 5: Calculated Geometry Parameters and Uranyl Frequencies of $[UO_2(H_2O)_5]^{n+}$, $n = 1, 2$, for Different Levels of Explicit Solvation (Priroda Four-Component Scalar and ADF-ZORA-COSMO PBE Calculations; Bond Lengths in Å, Frequencies in cm^{-1})

	$[UO_2(H_2O)_5]^{2+}$		$[UO_2(H_2O)_5]^{2+}\cdot 5H_2O$		$[UO_2(H_2O)_5]^{2+}\cdot 7H_2O$		$[UO_2(H_2O)_5]^{2+}\cdot 10H_2O$		$[UO_2(H_2O)_5]^{2+}\cdot 12H_2O$		
	gas phase	solvated[c]	gas phase	solvated[c]	gas phase	solvated[c]	gas phase	solvated[c]	gas phase	solvated[c]	Exp.[a]
R(U═O)	1.778	1.782, 1.781	1.784	1.797	1.802, 1.790	1.803, 1.799	1.816, 1.794	1.802, 1.810	1.817	1.816, 1.818	1.76, 1.78
$R(An{-}O_{eq})$[b]	2.482	2.410	2.468	2.436	2.444	2.430	2.437	2.429	2.388	2.410	2.41
ν_{symm}	898		883		856		840		822, 816 [d]		870, 869
ν_{asym}	991		974		967		954		898, 890[d]		965, 962
	$[UO_2(H_2O)_5]^{1+}$		$[UO_2(H_2O)_5]^{1+}\cdot 5H_2O$		$[UO_2(H_2O)_5]^{1+}\cdot 7H_2O$		$[UO_2(H_2O)_5]^{1+}\cdot 10H_2O$		$[UO_2(H_2O)_5]^{1+}\cdot 12H_2O$		
	gas phase	solvated[c]	gas phase	solvated[c]	gas phase	solvated[c]	gas phase	solvated[c]	gas phase	solvated[c]	
R(U═O)	1.826	1.844	1.866	1.867	1.885, 1.853	1.883, 1.861	1.856, 1.905	1.861, 1.887	1.894, 1.910	1.889	
$R(An{-}O_{eq})$[b]	2.587	2.566	2.579	2.566	2.546	2.538	2.524	2.532	2.506	2.523	
ν_{symm}	823		770		745		708, 720[d]		703, 724[d]		
ν_{asym}	883		862		790, 828		-[d]		786[d]		

[a] Experimental data[1−3,6,9] cited from Hay et al.[20] [b] Average. [c] Bulk solvation effects estimated with the COSMO method (ADF). [d] These vibrations are strongly coupled with ligand modes.

TABLE 6: Energy of the Uranyl Half Reaction $[UO_2]^{2+} + e^- \rightarrow [UO_2]^{1+}$, Reaction 3, for Different Levels of Water Coordination (Gas-Phase Priroda-TZP Four-Component Scalar and ADF-ZORA-COSMO PBE Calculations)

	ΔE U^{VI}/U^{V} (eV)		
complex	gas phase	COSMO solvation, gas-phase geometries	COSMO solvation, COSMO-optimized geometries
bare UO_2^{n+}	−14.94	−4.22	−4.17
$[UO_2(H_2O)_5]^{n+}$	−9.78	−4.72	−4.72
$[UO_2(H_2O)_5]^{n+}\cdot 5H_2O$	−8.14	−4.27	−4.31
$[UO_2(H_2O)_5]^{n+}\cdot 7H_2O$	−8.47	−4.50	−4.43
$[UO_2(H_2O)_5]^{n+}\cdot 10H_2O$	−8.28	−4.57	−4.46
$[UO_2(H_2O)_5]^{n+}\cdot 12H_2O$	−8.08	−4.58	−4.50

These (gas-phase) calculations were done using the four-component scalar relativistic method Priroda-TZP. Here, it is imperative to use a more extensive basis set than the DZP basis employed elsewhere in this paper to describe the relatively weak intermolecular interactions between the uranyl complex and the second solvation sphere. Moreover, we have included in Tables 5 and 6 calculations of the various explicitly solvated species under the presence of the bulk solvent as modeled by the COSMO solvation model.[68] We did not intend to cover the entire conformational space, or to search for the global energy minimum and because of that, the calculated energies will have some uncertainties. Nevertheless, a number of conclusions can be drawn.

Let us start with a qualitative discussion of the explicitly solvated complexes. Figure 2 shows the (gas-phase)-optimized structures for some of the U^{VI} complexes containing water molecules in the second coordination sphere. Upon inspection of these structures, it is evident that the uranyl (VI) oxygens are not prone to forming hydrogen bonds. Instead, the solvent molecules that were attached to these oxygens in the starting structure for the seven-water complex shift to the equatorial positions where they form part of the extended hydrogen-bond network around the equatorial ligands. The twelve-water complex shows one hydrogen bond per uranyl oxygen, after each of the hydrogen atoms in the first solvation sphere is saturated with its corresponding solvent molecule. The situation is slightly different for the U^{V} species. The uranyl bond is weaker in this case. This goes along with a larger negative charge at the uranyl oxygens, and therefore stronger tendency of these axial ligands to participate in the hydrogen bond network with the solvent.

To exploit this observation (and to collect more data on clusters of different size as well) we then performed calculations on the clusters with the two waters originally coordinated to the uranyl oxygens removed, i.e., with 5 and 10 water molecules in the second solvation sphere, $[UO_2(H_2O)_5]^{n+}\cdot 5H_2O$ and $[UO_2(H_2O)_5]^{n+}\cdot 10H_2O$, correspondingly. Figure 3 shows the optimized structures with five waters in the second coordination sphere. Interestingly, for the uranium(V) complexes, the water moleculess prefer to move back to form hydrogen bonds with the uranyl oxygen. This is illustrated in Figure 3b for $[UO_2(H_2O)_5]^{n+}\cdot 5H_2O$. Complexes of uranium(VI) do not do that, as can be seen in Figure 3a.

Calculated and experimental[1−3,6,9] bond lengths and uranyl frequencies are summarized in Table 5. We notice the following trends. Explicit solvation beyond the first coordination sphere leads to decreased equatorial bond lengths. Recalling the earlier discussion of the (gas-phase) bond lengths, we note that the equatorial bond lengths were overestimated by all methods. These are improved considerably in the microsolvated structures (clusters) as is evident for the U^{VI} species where experimental bond lengths are available. Explicit (cluster) solvation leads to longer axial bond lengths, and an accompanying decrease in the respective harmonic frequencies. For the PBE (Priroda four-component scalar) calculations shown in Table 5, this leads to increased deviations from experiment, at least for the U^{VI} species. However, we had noted earlier that the B3LYP calculations led to (gas-phase) overbinding along the uranyl axis, Table 1. It is expected that the trend shown in Table 5 would be similar for SC-ECP-B3LYP calculations, which then would improve the uranyl bond lengths and frequencies, rather then worsen them, as is the case for the PBE calculations.

Including effects of the bulk solvent by means of the COSMO model[68] leads to contraction of the equatorial bond lengths by, on average, 0.07 Å for the $[UO_2(H_2O)_5]^{2+}$ species, leading to excellent agreement with the experimental data. The bulk solvent has much less influence on the axial bond lengths or the equatorial bond lengths in the explicitly solvated systems. The influence is markedly smaller for the uranyl(V) species than

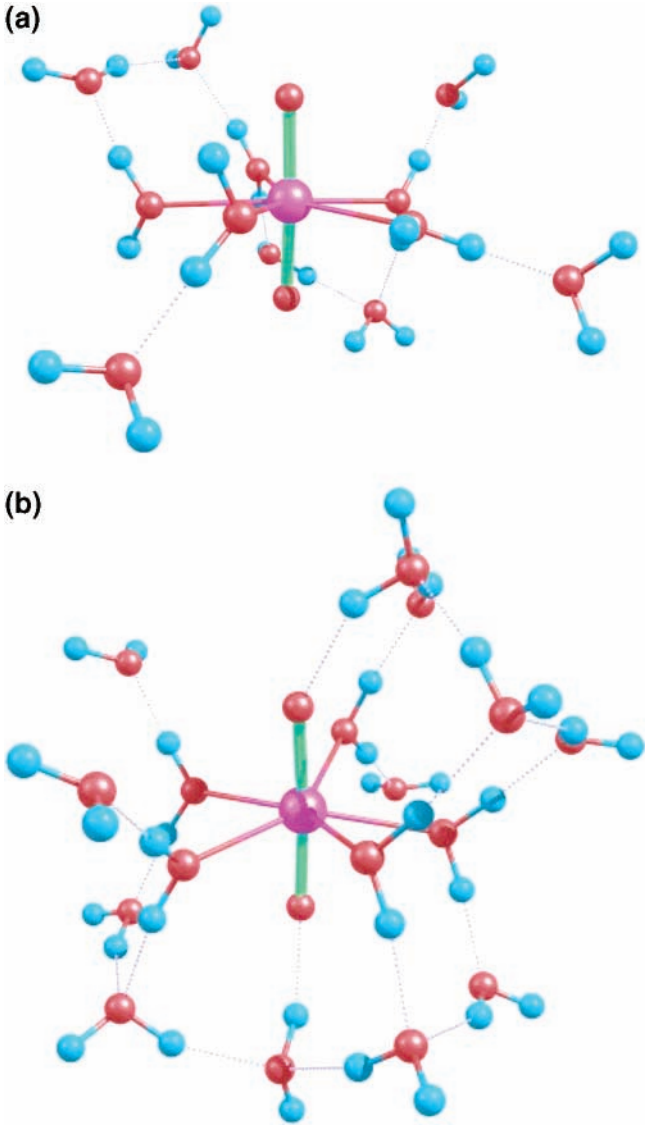

Figure 2. Optimized structure of the solvated U^{VI} complexes (a) $[UO_2(H_2O)_5]^{2+}\cdot 7H_2O$ and (b) $[UO_2(H_2O)_5]^{2+}\cdot 12H_2O$.

for the uranyl(VI) complex. This can be readily understood from the smaller charge, 1+ vs 2+ for the uranyl(VI) systems.

Overall, it appears as though the equatorial bond lengths that were overestimated by gas phase calculations (Table 1, see above) are correctly reproduced by either explicit or implicit solvation—both methods give similar bond lengths. On the other hand, combining microsolvation with continuum solvation (i.e., embedding the larger clusters into the continuum model for the remainder of the solvent) leads to slightly fluctuating results for the bond lengths, with no monotonic trend apparent. However, in all cases, the bond lengths are closer to experiment than the pure gas-phase ones, Table 5.

Table 6 provides the electronic energy ΔE for the uranyl half-reaction

$$[UO_2]^{2+} + e^- \rightarrow [UO_2]^{1+} \qquad (3)$$

Let us start again with the explicitly solvated models (gas-phase calculations). Not surprisingly, the first coordination sphere has a strong influence on this energy, as seen from the gas-phase calculations. Adding waters to the second coordination sphere leads to changes between 1.3 and 1.7 eV. However, the effect of the bulk solvent (as modeled with the COSMO[68] method) is much larger, and amounts to between 10.7 eV for the bare uranyl and 3.5 eV for $[UO_2(H_2O)_5]^{n+}\cdot 12H_2O$. Thus, the supermolecular approach (microsolvation) appears to be unable to capture the solvent response in its entirety. However, when COSMO solvation is included, the energy corresponding to eq 3 is relatively stable upon inclusion of second-coordination-sphere water molecules. Thus, COSMO appears to capture the major part of the solvent effect. Reoptimizing the structures in the presence of the bulk solvent has relatively little influence on their total energies and therefore the reaction energy of eq 2, see Table 6. (For the biggest cluster with twelve water molecules in the second coordination sphere, the total energy was lowered by 5.3 kcal/mol for uranium(VI) and 3.4 kcal/mol for uranium(V) complexes due to COSMO optimization. The effect is smaller for the other species.)

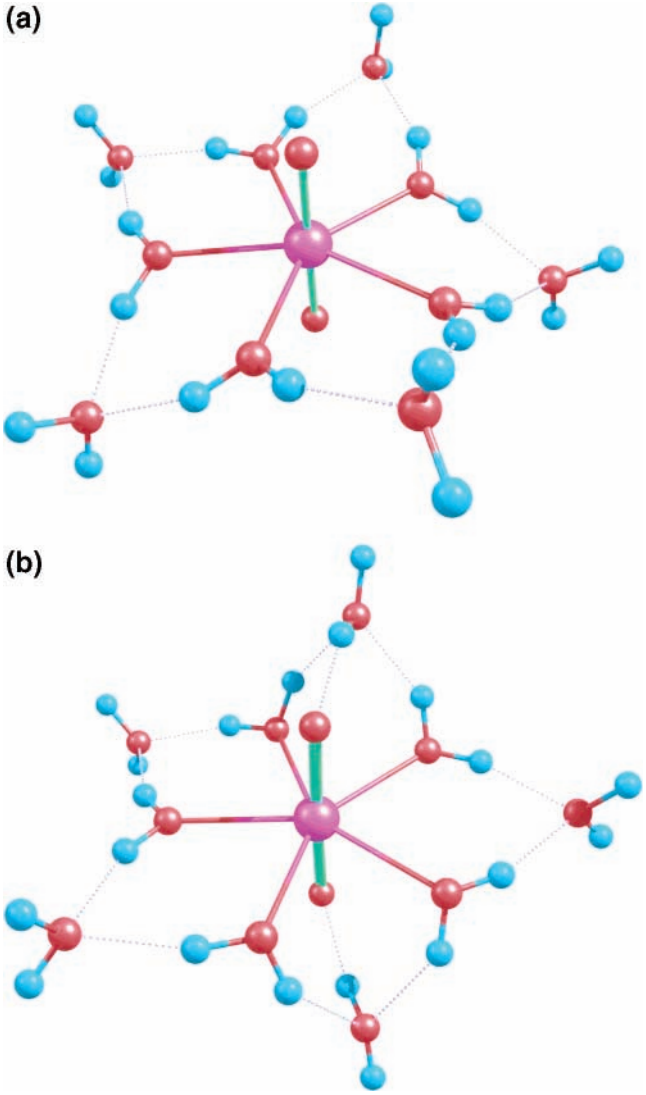

Figure 3. Optimized structure of the solvated uranium complexes (a) $[U^{VI}O_2(H_2O)_5]^{2+}\cdot 5H_2O$ and (b) $[U^{V}O_2(H_2O)_5]^{+}\cdot 5H_2O$.

We will come back to the An^{VI}/An^{V} reduction potential below.

Free Energy of Hydration. A further test for our solvation models is provided by calculating the free energies of hydration according to the reaction

$$AnO_2^{n+} + 5H_2O\ (aq) \rightarrow [AnO_2(H_2O)_5]^{n+}\ (aq)\ (n = 1, 2) \qquad (4)$$

The free energy of hydration of the uranyl(VI) ion UO_2^{2+} has

TABLE 7: Energies of Hydration of the Uranyl Cations with Different Solvation Models (Gas-Phase Priroda TZP Four-Component Scalar and ADF-ZORA-COSMO PBE calculations; in kcal/mol); Energies Correspond to the Following Reaction: $UO_2^{n+} + mH_2O \rightarrow [UO_2(H_2O)_l]^{n+}\cdot(m-l)H_2O$; $l = 0$ for Bare UO_2^{n+} and $l = 5$ Otherwise, and m Independent Water Molecules (Values in Parenthesis Are Calculated Relatively to the $(H_2O)_m$ Clusters, See Text for Details)

complex	ΔG_{298} gas phase[a]		$\Delta\Delta G^{solv}$ COSMO, gas-phase geometries[b]		$\Delta\Delta G^{solv}$ COSMO, solvation-optimized geometries[b]		ΔG_{298}^{hydr} COSMO, salvation-optimized geometries		ΔG_{298}^{hydr} corrected[c]
bare UO_2^{2+}	0.0		−462.6		−467.5		−467.5		
$[UO_2(H_2O)_5]^{2+}$	−197.8	(−208.1)	−163.5	(−178.2)	−164.6	(−179.0)	−362.4	(−387.0)	−383.89
$[UO_2(H_2O)_5]^{2+}\cdot 5H_2O$	−246.3	(−243.8)	−133.1	(−143.3)	−135.8	(−144.8)	−382.1	(−388.6)	−425.1
$[UO_2(H_2O)_5]^{2+}\cdot 7H_2O$	−263.9	(−252.2)	−88.0	(−141.3)	−92.3	(−144.5)	−356.2	(−396.7)	−407.83
$[UO_2(H_2O)_5]^{2+}\cdot 10H_2O$	−278.8	(−260.3)	−67.8	(−133.4)	−72.7	(−136.7)	−351.5	(−397.0)	−415.9
$[UO_2(H_2O)_5]^{2+}\cdot 12H_2O$	−285.4	(−265.8)	−51.8	(−125.0)	−57.1	(−128.3)	−342.5	(−394.1)	−415.58
Bare UO_2^{+}	0.0		−220.0		−224.0		−224.0		
$[UO_2(H_2O)_5]^{+}$	−79.4	(−74.9)	−43.0	(−57.7)	−43.8	(−58.2)	−123.3	(−133.1)	−144.78
$[UO_2(H_2O)_5]^{+}\cdot 5H_2O$	−96.4	(−85.9)	−43.0	(−53.2)	−43.8	(−55.4)	−123.3	(−141.3)	−153.1
$[UO_2(H_2O)_5]^{+}\cdot 7H_2O$	−107.5	(−95.8)	7.4	(−46.0)	4.7	(−47.5)	−102.8	(−143.2)	−154.4
$[UO_2(H_2O)_5]^{+}\cdot 10H_2O$	−116.5	(−100.2)	22.2	(−43.3)	20.0	(−44.0)	−96.5	(−144.1)	−161.0
$[UO_2(H_2O)_5]^{+}\cdot 12H_2O$	−120.2	(−100.6)	32.7	(−40.5)	29.3	(−42.0)	−90.9	(−142.5)	−164.0

[a] Priroda-PBE calculations. [b] ADF-COSMO-PBE calculations, $\Delta\Delta G^{solv} = \Delta G^{solv}(\text{complex}) - m\Delta G^{solv}(H_2O)$. [c] Translational entropy of water decreased, see text.

been studied earlier by Moskaleva et al.[33] Here, we extend these studies to Np and Pu, as well as to the respective An^V species. Moreover, we use the free energies of hydration as a further test of our theoretical models that differ from those used by Moskaleva et al.[33]

The free energy of reaction 4 can be calculated in two different ways. We can consider the five water molecules forming the first coordination sphere (or the $5 + k$ waters forming the first and second coordination spheres) as independent and treat them as separate molecules that are solvated as modeled by a continuum model. Alternatively, we can perform a gas-phase optimization of a cluster of these water molecules and calculate the bulk solvent effects for this cluster using a continuum model. We will explore and compare both procedures below.

First, we explore the effects of the first and second coordination spheres on uranyl(V) and (VI) within the COSMO continuum model using the "independent waters" approach. The corresponding gas-phase free energies of the reaction 4, ΔG_{298}, the changes in free energies due to COSMO solvation, $\Delta\Delta G^{solv}$, and the total hydration free energies ΔG_{298}^{hydr} are provided in Table 7 for the bare uranyls, the penta-aquo complexes, and clusters of the latter with 5, 7, 10, and 12 waters in the second coordination sphere. Results are provided for both single-point calculations and reoptimization within COSMO. The difference in the corresponding energies due to reoptimization in the solvent phase is not significant (Table 7).

Solvation energies are high for bare uranyls within COSMO-modeled water, Table 7. Inclusion of the five first solvation sphere waters lowers the solvation energy, as well as the total hydration free energy.

Inclusion of water molecules in the second coordination sphere further decreases the hydration energies (calculated using the "independent waters" scheme), Table 7. When more waters are added, the gas-phase binding energy ΔG_{298} of the uranyl-including cluster increases slower than the COSMO solvation energy ΔG^{solv} falls with the explicit inclusion of water molecules, as one should expect. However, accounting for the standard-state correction for the translation entropy of the each individual water molecule will make ΔG_{298}^{hydr} rise again, since the correction is proportional to the number of water molecules.

The free energy of hydration of uranyl can also be calculated by the alternative "clustered water" approach as described above. This adds some further uncertainties due to many close lying configurations that are possible for the water clusters. Moreover, many possible combinations of water clusters of different sizes can be imagined. (For instance, which is preferable, a single 15-water cluster or three 5-water clusters?) A recent example of the application of a mixed cluster continuum solvation model and the "clustered water" scheme for a complexes of dichloroplatinum(II)[82] showed strong fluctuations in the solvation energies: an increase in the number of second solvation sphere waters from four to eight led to a 10 kcal/mol difference as compared to both four-water and pure-continuum schemes which were consistent with each other.

In our work, we did not aim to determine global minima for the either the clusters of water around uranyl species or the pure water clusters. In the literature, there are papers dealing with water clusters of medium size. Maheshwari et al.[83] optimized such clusters at the Hartree−Fock level of theory, and recently Lenz et al.[84] at the B3LYP level. It was shown that the most stable water clusters are those formed from pentagonal or cubical substructures. We have taken a number of the most stable cluster configurations for 5, 10, 12, 15, and 17 water molecules as published in refs 83 and 84 and reoptimized them with the Priroda-TZP-PBE method. The final structures we have taken for our thermochemistry calculations were clusters corresponding to structures 5, 10B, 12A, 15A, and 17B from Maheshwari's paper.[83] The gas-phase geometries of the water clusters were treated with ADF-COSMO using the same procedure as for microsolvated uranyl complexes. Resulting Gibbs free energies are provided in Table 7 in parentheses.

First, we note that the gas-phase ΔG_{298} does not grow as fast for the "clustered-waters" approach as it did for the "independent-waters". This is because now, ΔG_{298} includes water cluster binding energies. One could view this as a benefit as compared to the "independent-waters" scheme because it can somewhat cancel out errors arising from the DFT treatment of the finite-size clusters. $\Delta\Delta G^{solv}$, which is now the change in solvation energy due to placing a uranyl cation into a solvated water cluster, is now more negative. It increases (i.e., gets less negative) with increasing cluster size, but this increase is slower than for the "independent-waters" approach. Thus, the total hydration free energies obtained by the method do not decrease (although they fluctuate slightly). They look reasonably converged (Table 7), unlike those reported by Hush et al.[82] for neutral platinum complexes. The difference between 7 and 12 waters in the second coordination sphere is now about 2 kcal/mol. The hydration energies are between corrected and uncorrected results obtained in the "independent-waters" approach

TABLE 8: Gibbs Free Energies of Hydration (Eq 3) and Contributions Thereof, G03 SC-ECP−B3LYP and *(italic, in brackets)* Priroda DZP Four-component PBE Calculations. Energies in kcal/mol; Entropies in cal/(mol K)

	calculated				experimental		
	ΔG_{298} gas phase	$\Delta\Delta G^{solv}$ [a]	ΔG_{298}^{hydr}	ΔG_{298}^{hydr} corrected	ΔH^{hydr} [b]	ΔS^{hydr} [c]	ΔG_{298}^{hydr} [c]
UO_2^{2+}	−224.9	−167.7	−392.0	−413.5	−397.9	78.6	−421.4
	(−192.1)	*(−169.8)*	*(−361.9)*	*(−383.4)*			
UO_2^{1+}	−106.0	−43.7	−149.7	−171.2	−169.5	0.0	−169.5
	(−68.5)	*(−47.5)*	*(−116.0)*	*(−137.4)*			
NpO_2^{2+}	−223.2	−168.0	−391.1	−412.6	−399.1	78.6	−422.6
	(−187.3)	*(−171.0)*	*(−358.2)*	*(−379.7)*			
NpO_2^{1+}	−113.0	−41.1	−154.1	−175.6	−180.2	0.0	−180.2
	(−64.0)	*(−45.7)*	*(−109.7)*	*(−131.2)*			
PuO_2^{2+}	−220.1	−167.8	−387.9	−409.4	−399.4	78.6	−422.8
	(−183.8)	*(−171.5)*	*(−355.3)*	*(−376.8)*			
PuO_2^{1+}	−105.0	−41.8	−146.8	−168.3	−178.3	0.0	−178.3
	(−62.6)	*(−43.9)*	*(−106.5)*	*(−128.0)*			

[a] CPCM continuum solvation model. For Priroda calculations, $\Delta\Delta G^{solv}$ from Gaussian calculations applied. Definition of $\Delta\Delta G^{solv}$and ΔG_{298}^{hydr} as in footnotes to Table 7. [b] Reference 18. [c] Estimate based on data from refs 85, 86 for UO_2^{2+}; we assume that the entropy of solvation is the same for the neptunyls and plutonyls.

and closer to the corrected ones. We believe that for the "clustered-waters" model the standard-state corrections can be neglected since water molecules forming clusters do not have the extra translational freedom. The correction for the entire cluster will be equal to or smaller than that for a single water molecule, and it will decrease with the size of the cluster. Thus, the correction would not influence the convergence of hydration energies with respect to cluster size.

Comparing theory and experiment is not straightforward in this case. In a recent article,[18] accurate experimental enthalpies of hydration are provided for uranyl, neptunyl, plutonyl, and americyl mono- and dications, derived from mass-spectrometric and thermochemical measurements. However, the result of calculations with continuum solvation models such as CPCM or COSMO is essentially a free energy, not an enthalpy. Deriving the enthalpy and entropy contributions from it—although possible by differentiation of the free energy with respect to temperature—poses severe methodological problems.[70] Thus, we have estimated the experimental free energies of hydration of uranyls by using the enthalpies according to the recent data by Gibson et al.,[18] as well as entropy contributions as estimated by Marcus et al.[85,86] The latter references provide data only for the uranium (VI) species (−78.6 cal/(mol K)). No experimental entropy of hydration is available for uranyl-(V) or for the other actinyl(V) species. However, it is known[86] that monocations usually have higher (i.e., less negative) values for the hydration entropy than dications of comparable nature. By that analogy, we expect ΔS_{298}^{hydr} for actinyl(V) species to be approximately 0 cal/(mol K). We therefore estimate the hydration Gibbs free energies of actinyl(V) species to be equal to the corresponding enthalpies. All of the above gives us "experimental" values for ΔG_{298}^{hydr} equal to −421.4 and −169.5 kcal/mol for the uranyl(VI) and (V), respectively. The values have error bars about ±15 kcal/mol.

Let us compare the values of calculated hydration Gibbs energies in Table 7 against these estimated experimental values. In agreement with the findings of Moskaleva et al.[33] for U^{VI}, one can see that the COSMO energies of bare uranyls are overestimated. Explicit inclusion of the five water molecules in the first coordination sphere greatly improves hydration energies, although they are now underestimated as compared to experiment. For the "independent-waters" scheme, there is agreement with the experiment in the case of the $[UO_2(H_2O)_5](H_2O)_{12}^{n+}$ complexes (although the convergence with respect to the number of water molecules is not yet known.) The "clustered-waters" scheme shows results that are slightly underestimated as compared to experiment but seems converged at $[UO_2(H_2O)_5](H_2O)_7^{n+}$. Thus, both schemes of calculation seem to show comparable results; including the second solvation sphere of the complexes leads to Gibbs free energies of hydration that are more negative as compared to first-sphere only calculation by a few tens of kcal/mol. It should be noted that the effect of the second coordination sphere is fairly systematic and of similar value for both uranium(VI) and (V) complexes, which means that for the calculations of the An^{VI}/An^{V} reduction potentials (see below) these effects would cancel out.

We conclude that the most practical solvation model should comprise gas-phase-optimized actinyl complexes including the water molecules of the first solvation sphere combined with a continuum solvation model for the remainder of the solvent.

The free energies of hydration for all the An^{V} and An^{VI} species calculated with that model are shown in Table 8. For simplicity, we use the "independent-waters" scheme of calculations, so the corrections to the Gibbs free energies must be applied. We have also included the various contributions, as well as the experimental values.[18,85,86]

As was mentioned above, there are no experimental hydration entropies available for the neptunyls and plutonyls, neither An^{VI} nor An^{V}. However, we assume transferability along the series from U to Np and Pu and thus take the values from the corresponding uranium complexes. This is reasonable because, on one hand, the entropy contributions are determined by vibrational degrees of freedom and, on the other hand, the structures of the hydrated complexes are rather similar for all three actinides. The "experimental" values shown in Table 8 were estimated in that manner.

By assumption that our procedure for estimating the experimental free energies of hydration is correct, we see that it is the same for the three An^{VI} species and varies within the experimental error bar for the An^{V} complexes. This is borne out by the calculations. For the An^{VI} species, we get free energies that vary by less than 4 kcal/ mol for the SC-ECP-B3LYP calculations (less than 7 kcal/mol for the four-component-scalar PBE results). Likewise, the calculated free energy of hydration is essentially constant for the three An^{V} species, with variations of less than 10 kcal/mol along the series.

By comparison of theory and experiment, we note that the final (i.e. translational entropy corrected) B3LYP results are very close to experiment, especially given the experimental uncertainty arising from the procedure described above. The PBE method underestimates the free energies by some about 30−40

TABLE 9: Contributions to the Calculated An^{VI}/An^{V} Reduction Potentials for the Actinyl Half Reactions $[AnO_2(H_2O)_5]^{2+} + e^- \rightarrow [AnO_2(H_2O)_5]^{1+}$ (eV)

	G03 SC-ECP PBE, G03 B3LYP geometry		G03 SC-ECP PBE, Priroda geometry		Priroda DZP four-component scalar PBE, Priroda geometry			multiplet and spin-orbit corrections[c]
	ΔE (gas phase)	$\Delta(\Delta G^{solv})$[a]	ΔE (gas phase)	$\Delta(\Delta G^{solv})$[a]	ΔE (gas phase)	ΔG^{298} (gas phase)	ΔG^{298} (solvation)[b]	
U^{VI}/U^{V}	−9.90	5.38	−9.47	5.31	−9.55	−9.68	−4.38	−0.31
Np^{VI}/Np^{V}	−10.91	5.50	−10.40	5.43	−10.39	−10.34	−4.90	−1.17
Pu^{VI}/Pu^{V}	−11.41	5.47	−10.95	5.53	−10.90	−10.95	−5.42	−0.21

[a] Difference between ΔG^{298} in the gas phase and including CPCM solvation. $\Delta(\Delta G^{solva}) = \Delta\Delta G^{solv}(U^{V}) - \Delta\Delta G^{solv}(U^{VI})$ is the difference in $\Delta\Delta G^{solv}$ between product and reagent of the reduction half reaction. [b] $\Delta(\Delta G^{solv})$ from G03 SC-ECP−PBE calculations added to ΔG^{298} (gas phase). [c] Empirical corrections taken from ref 20.

TABLE 10: Calculated (G03 SC-ECP-B3LYP and LC-ECP-B3LYP and Priroda DZP Four-Component PBE) and Experimental An^{VI}/An^{V} Reduction Potentials Relative to the Standard Hydrogen Potential (Numbers in eV)[a]

		Priroda PBE		G03 SC-ECP B3LYP		LC-ECP B3LYP[d]
	experiment[b]	uncorrected[c]	corrected[c]	uncorrected[c]	corrected[c]	corrected[c]
U^{VI}/U^{V}	0.06	−0.82	−0.51	−0.41	−0.10	2.37
Np^{VI}/Np^{V}	1.14	−0.30	0.87	0.55	1.72	4.00
Pu^{VI}/Pu^{V}	0.91	0.22	0.43	1.08	1.29	3.28

[a] For the water half reaction $H_3O^+ + e^- \rightarrow 1/2H_2 + H_2O$ (standard hydrogen electrode), we used the following calculated reduction potentials: −4.93 (B3LYP) and −5.20 eV (PBE). [b] Experimental data[87] cited from ref 20. [c] Without "uncorrected" and with "corrected" spin−orbit and multiplet corrections (as listed in Table 7). [d] Reference 20. The calculated reduction potential for the water half reaction is −4.92 eV in this case.

kcal/mol as compared to B3LYP; the reason for this deviation lies purely in the gas-phase complex binding energies.

We note that, since the inclusion of the second coordination sphere would make the values more negative, the B3LYP results could slightly worsen as compared to the experiment whereas PBE could get better.

Reduction Potential. A central goal of the current paper is the prediction of the $[AnO_2(H_2O)_5]^{2+}/[AnO_2(H_2O)_5]^{1+}$ reduction potentials for the series of complexes of uranium, neptunium, and plutonium. Previously, we had studied them[20] using LC-ECP-B3LYP and the BSJ continuum solvation model. Moskaleva et al.[33] studied a reduction reaction involving a protonated uranyl(V) dicationic form to avoid solvation effects arising from the change in charge of the complex during reduction. However, we feel that there is no real need for using such rather artificial model systems; in the previous section, we have shown that our solvation methods give very reasonable results for both mono- and dications of actinyls. In the following calculations, we use actinyl penta-aquo complexes the bulk water solvent modeled by the CPCM continuum model.

The respective data has been collected in Tables 9 and 10 where we have also included the previous LC-ECP calculations that showed a systematic error of some 2−3 eV. The reduction potentials relative to the standard hydrogen electrode are also given in Figure 4.

By comparison of the older LC-ECP-B3LYP results with the current SC-ECP-B3LYP and four-component Priroda-PBE calculations (Table 10), we notice that the agreement with experiment[87] has been improved considerably. The LC-ECP-B3LYP numbers exhibit a systematic error of 2−3 eV. However, the deviations between either the SC-ECP or four-component (Priroda) results and experiments are reduced to less than 0.6 eV for both, the B3LYP and PBE XC functionals. The errors for B3LYP have now either sign, i.e., no systematic shift is apparent anymore, whereas the PBE reduction potentials are lower than the experimental values.

The ad hoc multiplet and spin−orbit corrections of Hay et al.[20] (listed in Table 9) are seen to be crucial in reproducing the experimentally observed trend in the reduction potential (viz., Np > Pu > U). Without these corrections, we obtain a uniform

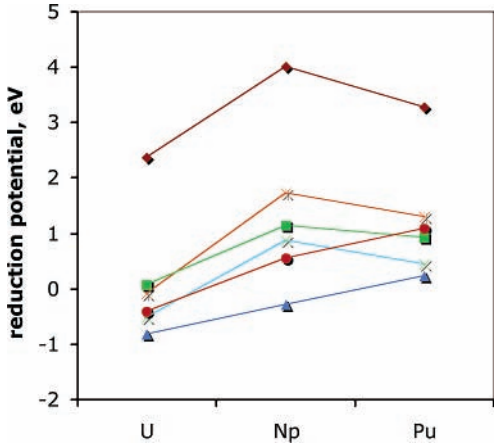

Figure 4. Calculated and experimental $[AnO_2(H_2O)_5]^{2+}/[AnO_2(H_2O)_5]^{1+}$ reduction potentials according to Table 10. Calculated values without and with the inclusion of spin−orbit and multiplet corrections are shown; see text. (Dark red diamonds) LC-ECP-B3LYP values from ref 20; (red circles and blue triangles) SC-ECP-B3LYP and Priroda-PBE values without the corrections; (orange stars and light blue crosses) SC-ECP B3LYP and Priroda PBE values with the corrections applied, correspondingly; (green squares) experimental values[87] as cited from ref 20.

increase in reduction potential with increasing atomic number, Table 10 and Figure 4.

To exclude as an error source the specifics of the particular LC-ECPs used in our earlier paper,[37] we have also recalculated the $[UO_2(H_2O)_5]^{2+}/[UO_2(H_2O)_5]^{1+}$ reduction potential using two further LC-ECPs. Not surprisingly, they give very similar results to those discussed above (when keeping all other settings, ligand basis sets, XC functional, solvation model, etc., the same.) For instance, the electronic contribution ΔE U^{VI}/U^{V} (gas phase) amounts to −11.4 and −11.8 eV for the SDD LC-ECPs[38] and CRENBL LC-ECPs,[88] respectively, which can be compared to a value of −12.1 eV obtained by us earlier.[20]

Conclusion

In this paper, we have studied the actinyl water complexes $[AnO_2(H_2O)_5]^{n+}$, $n = 1$ or 2 and An = U, Np, or Pu. Apart

from testing different approximations (see below), there are two main "chemical" results: Contrary to previous attempts, we have been able to accurately reproduce the An^{VI}/An^{V} reduction potential (Figure 4, Table 10). For the first time, we have calculated the free energies of hydration for all six species (eq 4, Table 8). The calculated free energies are within the experimental error bars in all cases.

In modeling complexes of the early actinide elements, approximations have to be chosen for at least four different principal effects. These are (i) relativity, (ii) electron correlation (in many cases this means choosing an approximate DFT method), (iii) solvation, and (iv) model complexes that contain truncated versions of the experimental ligands. In this article, we have evaluated different approximations in the first three areas. We have taken a general approach of applying as many different methods as possible to a given question. This allows us to compare the different methods, to exclude error compensation, and thus to verify one method with another. We will discuss these approximations in the following.

Relativity. For relativity, we have compared the older LC-ECP approach[20] to more modern methods including SC-ECP and a four-component scalar all-electron approach. We have also included spin−orbit (as well as multiplet) effects by utilizing an approximate, ad hoc approach.

In comparison of our older LC-ECP calculations[20] with the current SC-ECP results, we see that the latter method is clearly superior to the former for geometries, frequencies, and reduction potentials. Thus, we can add reduction potentials to the growing list of properties for which the SC-ECP approach significantly outperforms the LC-ECP one.

In more general terms, we have shown that two fundamentally different relativistic methods, SC-ECP (G03) and the all-electron scalar four-component method (Priroda), yield essentially similar results for a wide range of properties, provided all other approximations (notably the choice of approximate XC functional) are comparable. Indeed, experience shows that other methods, including the ZORA[63−66] and—presumably—the Douglas-Kroll-Hess (DKH) approach,[89,90] could be added here as well (although we have no direct experience with the latter). Thus, we can conclude that the question of the proper relativistic method for treating actinide molecules appears to be solved, as long as spin−orbit or deep-core effects are not relevant.

Spin−Orbit and Multiplet Effects. For spin−orbit and multiplet effects arising from the (formally nonbonding) f electrons, we have again used the ad hoc correction of Hay et al.[20] In this method, energy corrections arising from spin−orbit and multiplet effects are calculated using spin−orbit CI applied to bare plutonyl ions of different f^n occupations and charge. Applying such corrections assumes (i) transferability of Hartree−Fock-based SO-CI results to the DFT calculations (which, in particular, implies that approximate DFT does not account for the multiplet part of the correlation energy), (ii) negligible geometry influence, given that the SO-CI calculations employed a fixed geometry (although one could, in principle, repeat such calculations for different actinyl bond lengths), and (iii) a weak ligand field in the equatorial plane of the actinyl, i.e., transferability from the bare species to the complete complexes. These assumptions are rather severe and, as such, unsatisfactory from a theoretical point of view. However, as a pragmatic approach the method appears to work if our data is to be trusted as an indication. Thus, one might even consider extending this method to other types of actinide complexes (e.g., containing the lower oxidation states).

Solvation. We have extensively tested the continuum solvation models by studying various properties such as bond lengths and free energies of hydration. Testing of this sort is essential because it provides additional data points and thus excludes the possibility of error cancellation between the various levels of approximation (such as systematic errors in the relativistic approximation being partly compensated by errors in the solvation model.) The following conclusions emerge.

First, continuum solvation models such as COSMO or CPCM are reliable for the given purpose, and can be applied routinely. Second, our standard protocol of calculating single-point solvation energies based on gas-phase geometries is appropriate as far as energetics are concerned. Likewise, transferring solvation energies $\Delta\Delta G^{solv}$ from G03-based CPCM calculations to Priroda-based four-component applications appears to be justified. Third, the solvent environment has, however, a strong influence on the (equatorial) bond lengths. Accounting for the solvent environment either by continuum solvation models (COSMO) or by cluster models (microsolvation) is seen to be essential. Interestingly, either method seems to be appropriate, as far as bond lengths are concerned. However, the bond lengths appear to be not well described by the combination of the two methods, i.e., the embedded cluster model. Fourth, this is not the case for energetics where the long-range electrostatic effects of the bulk solvent have to be accounted for. Fifth, for energetics, inclusion of the first solvation sphere into continuum-modeled bulk water grasps the major part of the hydration free energy; additional second-sphere waters do improve the energy, but their influence is modest only. Sixth, we have tested both an "independent-water" and a "clustered-water" approach to modeling solvated water molecules. Both are seen to be roughly equivalent provided standard-state corrections are included in the former; these corrections are unnecessary for the latter.

XC Functional. We have compared two flavors of approximate DFT, hybrid DFT in the form of the B3LYP functional and a modern GGA in the form of PBE. The conclusions in this case are less clear-cut than for the relativistic method: Both approaches resulted in reduction potentials of similar quality but B3LYP is somewhat superior to PBE as far as the free energies of hydration are concerned. B3LYP apparently showed overbinding along the actinyl bonds, i.e., axial bond lengths that are too short and corresponding vibrational frequencies that are too high. These shortcomings are, to some degree, rectified by the GGA calculations. However, these conclusions are based on comparing gas-phase calculations to condensed-phase experimental data and are thus to be treated with some caution. Indeed, calculations that included explicit solvent molecules in the second coordination sphere (microsolvation) appear to indicate that solvent effects might rectify the problems of the B3LYP approach regarding bond lengths, while worsening the quality of the PBE uranyl frequencies.

Overall, the question of the best choice of approximate XC functional for actinide calculations is not solved, and further studies, preferably using accurate experimental gas-phase data, are required.

Acknowledgment. We are grateful to Dr. D. N. Laikov, Moscow/Stockholm, for making his Priroda code available to us. We appreciated the careful comments of two unknown referees. Financial support from the Natural Sciences and Engineering Research Council of Canada and from the University of Manitoba (start-up funds and University of Manitoba Research Grants Program) is gratefully acknowledged.

References and Notes

(1) Jones, L. H.; Penneman, R. A. *J. Chem. Phys.* **1953**, *21*, 542.

(2) Basile, L. J.; Sullivan, J. C.; Ferraro, J. R.; LaBonville, P. *Appl. Spectrosc.* **1974**, *28*, 142.

(3) Toth, L. M.; Begun, G. M. *J. Phys. Chem.* **1981**, *85*, 547.

(4) Madic, C.; Begun, G. M.; Hobart, D. E.; Hahn, R. L. *Inorg. Chem.* **1984**, *23*, 1914.

(5) Combes, J.-M.; Chisholm-Brause, C. J.; Brown, G. E., Jr.; Parks, G. A.; Conradson, S. D.; Eller, P. G.; Triay, I. R.; Hobart, D. E.; Meijer, A. *Environ. Sci. Technol.* **1992**, *26*, 376.

(6) Allen, P. G.; Bucher, J. J.; Shuh, D. K.; Edelstein, N. M.; Reich, T. *Inorg. Chem.* **1997**, *36*, 4676.

(7) Bardin, N.; Rubini, P.; Madic, C. *Radiochim. Acta* **1998**, *83*, 189.

(8) Conradson, S. D. *Appl. Spectrosc.* **1998**, *52*, 252A.

(9) Wahlgren, U.; Moll, H.; Grenthe, I.; Schimmelpfennig, B.; Maron, L.; Vallet, V.; Gropen, O. *J. Phys. Chem. A* **1999**, *103*, 8257.

(10) Farkas, I.; Banyai, I.; Szabo, Z.; Wahlgren, U.; Grenthe, I. *Inorg. Chem.* **2000**, *39*, 799.

(11) Antonio, M. R.; Soderholm, L.; Williams, C. W.; Blaudeau, J. P.; Bursten, B. E. *Radiochim. Acta* **2001**, *89*, 17.

(12) Den Auwer, C.; Simoni, E.; Conradson, S.; Madic, C. *Eur. J. Inorg. Chem.* **2003**, 3843.

(13) Gresham, G. L.; Gianotto, A. K.; Harrington, P. D.; Cao, L. B.; Scott, J. R.; Olson, J. E.; Appelhans, A. D.; Van Stipdonk, M. J.; Groenewold, G. S. *J. Phys. Chem. A* **2003**, *107*, 8530.

(14) Gianguzza, A.; Milea, D.; Millero, F. J.; Sammartano, S. *Mar. Chem.* **2004**, *85*, 103.

(15) Neuefeind, J.; Soderholm, L.; Skanthakumar, S. *J. Phys. Chem. A* **2004**, *108*, 2733.

(16) Semon, L.; Boehme, C.; Billard, I.; Hennig, C.; Lutzenkirchen, K.; Reich, T.; Rossberg, A.; Rossini, I.; Wipff, G. *Chemphyschem* **2001**, *2*, 591.

(17) Vallet, V.; Szabó, Z.; Grenthe, I. *J. Chem. Soc., Dalton Trans.* **2004**, 3799.

(18) Gibson, J. K.; Haire, R. G.; Santos, M.; Marçalo, J.; Pires de Matos, A. *J. Phys. Chem. A* 2005.

(19) Spencer, S.; Gagliardi, L.; Handy, N. C.; Ioannou, A. G.; Skylaris, C.-K.; Willets, A.; Simper, A. M. *J. Phys. Chem. A* **1999**, *103*, 1831.

(20) Hay, P. J.; Martin, R. L.; Schreckenbach, G. *J. Phys. Chem. A* **2000**, *104*, 6259.

(21) Blaudeau, J. P.; Zygmunt, S. A.; Curtiss, L. A.; Reed, D. T.; Bursten, B. E. *Chem. Phys. Lett.* **1999**, *310*, 347.

(22) Hemmingsen, L.; Amara, P.; Ansoborlo, E.; Field, M. J. *J. Phys. Chem. A* **2000**, *104*, 4095.

(23) Matsika, S.; Pitzer, R. M.; Reed, D. T. *J. Phys. Chem. A* **2000**, *104*, 11983.

(24) Tsushima, S.; Suzuki, A. *THEOCHEM* **2000**, *529*, 21.

(25) Tsushima, S.; Yang, T. X.; Suzuki, A. *Chem. Phys. Lett.* **2001**, *334*, 365.

(26) Vallet, V.; Wahlgren, U.; Schimmelpfennig, B.; Szabó, Z.; Grenthe, I. *J. Am. Chem. Soc.* **2001**, *123*, 11999.

(27) Yang, T. X.; Tsushima, S.; Suzuki, A. *J. Phys. Chem. A* **2001**, *105*, 10439.

(28) Fuchs, M. S. K.; Shor, A. M.; Rösch, N. *Int. J. Quantum Chem.* **2002**, *86*, 487.

(29) Greathouse, J. A.; O'Brien, R. J.; Bemis, G.; Pabalan, R. T. *J. Phys. Chem. B* **2002**, *106*, 1646.

(30) Oda, Y.; Aoshima, A. *J. Nucl. Sci. Technol.* **2002**, *39*, 647.

(31) Bridgeman, A. J.; Cavigliasso, G. *Faraday Discuss.* **2003**, *124*, 239.

(32) Clavaguera-Sarrio, C.; Brenner, V.; Hoyau, S.; Marsden, C. J.; Millie, P.; Dognon, J. P. *J. Phys. Chem. B* **2003**, *107*, 3051.

(33) Moskaleva, L. V.; Krüger, S.; Spörl, A.; Rösch, N. *Inorg. Chem.* **2004**, *43*, 4080.

(34) Vallet, V.; Privalov, T.; Wahlgren, U.; Grenthe, I. *J. Am. Chem. Soc.* **2004**, *126*, 7766.

(35) Koch, W.; Holthausen, M. C. *A Chemist's Guide to Density Functional Theory*; Verlag Chemie: New York, 2000.

(36) Schreckenbach, G.; Hay, P. J.; Martin, R. L. *J. Comput. Chem.* **1999**, *20*, 70.

(37) Hay, P. J.; Martin, R. L. *J. Chem. Phys.* **1998**, *109*, 3875.

(38) Küchle, W.; Dolg, M.; Stoll, H.; Preuss, H. *J. Chem. Phys.* **1994**, *100*, 7535.

(39) Han, Y.-K.; Hirao, K. *J. Chem. Phys.* **2000**, *113*, 7345.

(40) Han, Y. K. *J. Comput. Chem.* **2001**, *22*, 2010.

(41) Schreckenbach, G.; Wolff, S. K.; Ziegler, T. *J. Phys. Chem. A* **2000**, *104*, 8244.

(42) Schreckenbach, G. *Int. J. Quantum Chem.* **2005**, *101*, 372.

(43) Straka, M.; Kaupp, M. *Chem. Phys.* **2005**, *311*, 45.

(44) Batista, E. R.; Martin, R. L.; Hay, P. J.; Peralta, J. E.; Scuseria, G. E. *J. Chem. Phys.* **2004**, *121*, 2144.

(45) Becke, A. D. *J. Chem. Phys.* **1993**, *98*, 5648.

(46) Lee, C.; Yang, W.; Parr, R. G. *Phys. Rev. B: Condens. Matter* **1988**, *37*, 785.

(47) Stephens, P. J.; Devlin, F. J.; Chabalowski, C. F.; Frisch, M. J. *J. Phys. Chem.* **1994**, *98*, 11623.

(48) Infante, I.; Visscher, L. *J. Comput. Chem.* **2004**, *25*, 386.

(49) Frisch, M. J.; Trucks, G. W.; Schlegel, H. B.; Scuseria, G. E.; Robb, M. A.; Cheeseman, J. R.; Montgomery, J. A.; Vreven, T.; Kudin, K. N.; Burant, J. C.; Millam, J. M.; Iyengar, S. S.; Tomasi, J.; Barone, V.; Mennucci, B.; Cossi, M.; Scalmani, G.; Rega, N.; Petersson, G. A.; Nakatsuji, H.; Hada, M.; Ehara, M.; Toyota, K.; Fukuda, R.; Hasegawa, J.; Ishida, M.; Nakajima, T.; Honda, Y.; Kitao, O.; Nakai, H.; Klene, M.; Li, X.; Knox, J. E.; Hratchian, H. P.; Cross, J. B.; Bakken, V.; Adamo, C.; Jaramillo, J.; Gomperts, R.; Stratmann, R. E.; Yazyev, O.; Austin, A. J.; Cammi, R.; Pomelli, C.; Ochterski, J. W.; Ayala, P. Y.; Morokuma, K.; Voth, G. A.; Salvador, P.; Dannenberg, J. J.; Zakrzewski, V. G.; Dapprich, S.; Daniels, A. D.; Strain, M. C.; Farkas, O.; Malick, D. K.; Rabuck, A. D.; Raghavachari, K.; Foresman, J. B.; Ortiz, J. V.; Cui, Q.; Baboul, A. G.; Clifford, S.; Cioslowski, J.; Stefanov, B. B.; Liu, G.; Liashenko, A.; Piskorz, P.; Komaromi, I.; Martin, R. L.; Fox, D. J.; Keith, T.; Al-Laham, M. A.; Peng, C. Y.; Nanayakkara, A.; Challacombe, M.; Gill, P. M. W.; Johnson, B.; Chen, W.; Wong, M. W.; Gonzalez, C.; Pople, J. A. *Gaussian 03*; Gaussian, Inc.: Wallingford CT, 2004.

(50) Fonseca Guerra, C.; Snijders, J. G.; te Velde, G.; Baerends, E. *J. Theor. Chem. Acc.* **1998**, *99*, 391.

(51) te Velde, G.; Bickelhaupt, F. M.; Baerends, E. J.; Fonseca Guerra, C.; van Gisbergen, S. J. A.; Snijders, J. G.; Ziegler, T. *J. Comput. Chem.* **2001**, *22*, 931.

(52) Baerends, E. J.; A., A. J.; Bérces, A.; Bo, C.; Boerrigter, P. M.; Cavallo, L.; Chong, D. P.; Deng, L.; Dickson, R. M.; Ellis, D. E.; Fan, L.; Fischer, T. H.; Fonseca Guerra, C.; van Gisbergen, S. J. A.; Groeneveld, J. A.; Gritsenko, O. V.; Grüning, M.; Harris, F. E.; van den Hoek, P.; Jacobsen, H.; van Kessel, G.; Koostra, F.; van Lenthe, E.; McCormack, D. A.; Osinga, V. P.; Patchkovskii, S.; Philipsen, P. H. T.; Post, D.; Pye, C. C.; Ravenek, W.; Ros, P.; Schipper, P. R. T.; Schreckenbach, G.; Snijders, J. G.; Sola, M.; Swart, M.; Swerhone, D.; te Velde, G.; Vernooijs, P.; Versluis, L.; Visser, O.; van Wezenbeek, E.; Wiesenekker, G.; Wolff, S. K.; Woo, T. K.; Ziegler, T. *ADF 2004.01, Scientific Computing and Modelling, Theoretical Chemistry*; Vrije Universiteit: Amsterdam, The Netherlands, 2004.

(53) Laikov, D. N. *Chem. Phys. Lett.* **1997**, *281*, 151.

(54) Laikov, D. N. *An implementation of the scalar relativistic density functional theory for molecular calculations with Gaussian basis sets*; DFT2000 Conference, 2000, Menton, France.

(55) Laikov, D. N. Ph.D. Thesis, Moscow State University, 2000.

(56) Perdew, J. P.; Burke, K.; Ernzerhof, M. *Phys. Rev. Lett.* **1996**, *77*, 3865.

(57) Diri, K.; Myshakin, E. M.; Jordan, K. D. *J. Phys. Chem. A* **2005**, *109*, 4005.

(58) Hay, P. J. *Faraday Discuss.* **2003**, *124*, 69.

(59) Dyall, K. G. *J. Chem. Phys.* **1994**, *100*, 2118.

(60) Shamov, G. A.; Schreckenbach, G. To be published.

(61) Shamov, G. A.; Schreckenbach, G. *Theoretical Actinide Molecular Science with Relativistic Density Functional Theory*—Evaluation of Methods; 88th Canadian Chemistry Conference and Exhibition, 2005, Saskatoon, SK, Canada.

(62) Cossi, M.; Rega, N.; Giovanni, S.; Barone, V. *J. Comput. Chem.* **2003**, *24*, 669.

(63) van Lenthe, E.; Baerends, E. J.; Snijders, J. G. *J. Chem. Phys.* **1993**, *99*, 4597.

(64) van Lenthe, E.; Baerends, E. J.; Snijders, J. G. *J. Chem. Phys.* **1994**, *101*, 9783.

(65) van Lenthe, E.; van Leeuwen, R.; Baerends, E. *J. Int. Quantum Chem.* **1996**, *57*, 281.

(66) van Lenthe, E.; Ehlers, A.; Baerends, E. J. *J. Chem. Phys.* **1999**, *110*, 8943.

(67) Klamt, A.; Schüürmann, G. *J. Chem. Soc., Perkin Trans.* **1993**, *2*, 799.

(68) Pye, C. C.; Ziegler, T. *Theor. Chem. Acc.* **1999**, *101*, 396.

(69) Klamt, A.; Jonas, V.; Bürger, T.; Lohrenz, J. C. W. *J. Phys. Chem. A* **1998**, *102*, 5074.

(70) Martin, R. L.; Hay, P. J.; Pratt, L. R. *J. Phys. Chem. A* **1998**, *102*, 3565.

(71) van Lenthe, E.; Snijders, J. G.; Baerends, E. J. *J. Chem. Phys.* **1996**, *105*, 6505.

(72) Clavaguera-Sarrio, C.; Vallet, V.; Maynau, D.; Marsden, C. J. *J. Chem. Phys.* **2004**, *121*, 5312.

(73) Tatsumi, K.; Hoffmann, R. *Inorg. Chem.* **1980**, *19*, 2656.

(74) Wadt, W. R. *J. Am. Chem. Soc.* **1981**, *103*, 6053.

(75) Denning, R. G. *Struct. Bonding (Berlin)* **1992**, *79*, 215.

(76) Craw, J. S.; Vincent, M. A.; Hillier, I. H.; Wallwork, A. L. *J. Phys. Chem.* **1995**, *99*, 10181.

(77) Cornehl, H. H.; Heinemann, C.; Marçalo, J.; Pires de Matos, A.; Schwarz, H. *Angew. Chem., Int. Ed. Engl.* **1996**, *35*, 891.

(78) de Jong, W. A.; Harrison, R. J.; Nichols, J. A.; Dixon, D. A. *Theor. Chem. Acc.* **2001**, *107*, 22.
(79) Gagliardi, L.; Roos, B. O. *Inorg. Chem.* **2002**, *41*, 1315.
(80) Hummer, G.; Pratt, L. R.; Garcia, A. E. *J. Am. Chem. Soc.* **1997**, *119*, 8523.
(81) Miertus, S.; Scrocco, E.; Tomasi, *J. Chem. Phys.* **1981**, *55*, 117.
(82) Hush, N. S.; Schamberger, J.; Bacskay, G. B. *Coord. Chem. Rev.* **2005**, *249*, 299.
(83) Mahmeshwary, S.; Patel, N.; Sathyamurthy, N.; Kulkarni, A. D.; Gadre, S. R. *J. Phys. Chem. A* **2001**, *105*, 10525.
(84) Lenz, A.; Ojamae, L. *Phys. Chem. Chem. Phys.* **2005**, *7*, 1905.
(85) Marcus, Y. *Inorg. Nucl. Chem.* **1975**, *37*, 493.
(86) Marcus, Y. *Ion Solvation*; Wiley: New York, 1985.
(87) *Encyclopedia of Electrochemistry of the Elements*; Bard, A. J., Ed.; M. Dekker: New York, 1973; Vol. 8.
(88) Nash, C. S.; Bursten, B. E.; Ermler, W. C. *J. Chem. Phys.* **1997**, *106*, 5133.
(89) Douglas, M.; Kroll, N. M. *Ann. Phys.* **1974**, *82*, 89.
(90) Hess, B. A. *Phys. Rev. A* **1986**, *33*, 3742.